PB90-155557

Model of Turbulent Diffusion Flames and Nitric Oxide Generation

TRW Space and Technology Group, Redondo Beach, CA

Prepared for:

Environmental Protection Agency, Research Triangle Park, NC

Jan 90

U.S. Department of Commerce
National Technical Information Service
NTIS

BIBLIOGRAPHIC INFORMATION

PB90-155557

Report Nos: none

Title: Model of Turbulent Diffusion Flames and Nitric Oxide Generation.

Date: Jan 90

Authors: J. E. Broadwell, T. J. Tyson, and C. J. Kau.

Performing Organization: TRW Space and Technology Group, Redondo Beach, CA.**Energy and Environmental Research Corp., Irvine, CA.

Performing Organization Report Nos: EPA/600/7-90/003

Sponsoring Organization: *Environmental Protection Agency, Research Triangle Park, NC. Air and Energy Engineering Research Lab.

Contract Nos: EPA-68-02-3633

Supplementary Notes: Prepared in cooperation with Energy and Environmental Research Corp., Irvine, CA. Sponsored by Environmental Protection Agency, Research Triangle Park, NC. Air and Energy Engineering Research Lab.

NTIS Field/Group Codes: 81A, 68A

Price: PC A04/MF A01

Availability: Available from the National Technical Information Service, Springfield, VA. 22161

Number of Pages: 53p

Keywords: *Diffusion flames, *Turbulence, *Nitrogen oxide(NO), *Mixing, Combustion, Combustion products, Mathematical models, Flame propagation, Reaction kinetics, Chemical reactions, Experimental data.

Abstract: A new view is described of mixing and chemical reactions in turbulent fuel jets discharging into air. Review of available fundamental data from jet flames leads to the idea that mixing begins with a large scale, inviscid, intertwining of entrained air and fuel throughout the jet. Significant molecular mixing is delayed until the end of a cascade to the Kolmogorov scale. A simple mathematical model incorporating these ideas is presented. The model predicts a Reynolds number dependence for the nitric oxide formation rate that is in good agreement with measurements in both methane and hydrogen jets burning in air. These mathematical model concepts have been incorporated into a simplified computer program capable of treating the detailed chemical kinetics of a gas flame. The model has been used to predict NO formation in H2/air and CH4/air flames and results compare favorably with experimental data.

EPA-600/7-90-003
January 1990

A MODEL OF TURBULENT DIFFUSION FLAMES AND NITRIC OXIDE GENERATION

PB90-155557

by:

J.E. Broadwell
(TRW Space and Technology Group)

and

T.J. Tyson
C.J. Kau
Energy and Environmental Research Corporation
18 Mason
Irvine, CA 92718

EPA Contract 68-02-3633

EPA Project Officer

W. Steven Lanier
Air and Energy Engineering Research Laboratory
Research Triangle Park, NC 27711

Air and Energy Engineering Research Laboratory
Office of Research and Development
U. S. Environmental Protection Agency
Research Triangle Park, NC 27711

REPRODUCED BY
U.S. DEPARTMENT OF COMMERCE
NATIONAL TECHNICAL INFORMATION SERVICE
SPRINGFIELD, VA. 22161

#00

#01 PB90-155557

#02 Field 81A, 68A

#03 U034159

#23 Descriptors: *Diffusion flames, *Turbulence, *Nitrogen oxide(NO), *Mixing, Combustion, Combustion products, Mathematical models, Flame propagation, Reaction kinetics, Chemical reactions, Experimental data.

#27 A new view is described of mixing and chemical reactions in turbulent fuel jets discharging into air. Review of available fundamental data from jet flames leads to the idea that mixing begins with a large scale, inviscid, intertwining of entrained air and fuel throughout the jet. Significant molecular mixing is delayed until the end of a cascade to the Kolmogorov scale. A simple mathematical model incorporating these ideas is presented. The model predicts a Reynolds number dependence for the nitric oxide formation rate that is in good agreement with measurements in both methane and hydrogen jets burning in air. These mathematical model concepts have been incorporated into a simplified computer program capable of treating the detailed chemical kinetics of a gas flame. The model has been used to predict NO formation in H2/air and CH4/air flames and results compare favorably with experimental data.

#30 0

SOL

CONTROL NUMBER: 034159

BATCH NUMBER:

MGT. CD.

AN RV KY VR ED: C

ACCESSION NUMBER: PB90-155557

03A) ANN GRA WGA DB:

03G) GRAPHICS:

30A): Ø (0 N/A, 1 Ann-I, 2 R, 3 T, 4 FOR, 5 For-T, 6 For-R)

02S) SUBJECT CATEGORIES: 81A, 68A

23D) DESCRIPTORS

* Diffusion flames,
* Turbulence,
* Nitrogen oxide (NO),
* Mixing,
Combustion,
Combustion products,
Mathematical models,
Flame propagation,
Reaction kinetics,
Chemical reactions,
Experimental data,

25I) IDENTIFIERS

27A) ABSTRACT

PAGES: iii

BDS NONE BELOW

AN 89

FULL DOCUMENT PROCESSING

1. CONTROL NUMBER: U

BATCH NUMBER

3. COL. CD.

4. ACCESSION NUMBER

.. SOURCE CODE

2A. RECOGNITION NUMBER

10. TRANSACTION N NEW D DUPLICATE P PRIOR S SUPERSEDES

10A.

6. MGT. CD.: C D A R K V

7. PROCESS ACCTG. CD.

7A. REGISTRATION FEE

8. PROD. MGR.

9. RECEIPT TYPE
0 N/A 3 ERRATA
1 RETAIN 4 LOAN
2 LAST

9A. LOAN DUE OUT: Y Y D D D

11. PRICE
1. STD.
2. EXC.

12. RETURNS
0 N/A 5 REST.
1 PAGES 8 MISC.
3 REPRO
4 BDS

12A. RETURN DATE: Y Y M M D D

13. PROCESS
0 STANDARD 3 UNEDIT
1 INVENTORY 4 REANNOUNCE
2 HIGHLIGHT 5 SPECIAL BIB

14. PAT. POTENTIAL
0 NO 3 GOOD
1 POOR 4 EXCEL.
2 FAIR

16. BILL

17. FORM/PRICE

18. ANNOUNCE: GRA WGA D D/B

19. PUBLICATION-1: U

20. PUBLICATION-2

20A. PUBLICATION-3

21. LIMITATION
0 N/A
1 DISCLAIMER
2 COLOR
3 COMBO

23. PC BIN STOCK 24A. PAGES/SHEETS PRICE CODE DOMESTIC PRICE FOREIGN PRICE ACTION CD.

MICROFICHE
37. REL. CD. 38. MF PRINT

40. PRINT PC

43. 43A) ORDER ADD'L STOCK & CODE ADDR 43B) BIN MSG 43C) STK UNIT COST 43D) SET ID 43E) CAMERA CONTROL 43F) REFER TO ADDR

39. ADD. INFO.

41. PC DUE

42. SOURCE ORDER

42A NDP | N A I RDA Z | 42B. SUPPLIER SOURCE

COPYRIGHT
YES NO INITL.

RD _____

44. BATCH NO.

02C) COM. CAT.

03S) ADDITIONAL SOURCE CLIENTS

03L) LANGUAGE

03C) COMP. ENTRY CODE

34) SERIAL

35) CORP. AUTHOR CD.

U.S. AUTH.

MGT. CD.
CAT REV KEY VER

45. REMARKS (DO NOT KEY)

NOTICE

This document has been reviewed in accordance with U.S. Environmental Protection Agency policy and approved for publication. Mention of trade names or commercial products does not constitute endorsement or recommendation for use.

ABSTRACT

A new view is described of mixing and chemical reactions in turbulent fuel jets discharging into air. Review of available fundamental data from jet flames leads to the idea that mixing begins with a large scale, inviscid, intertwining of entrained air and fuel throughout the jet. Significant molecular mixing is delayed until the end of a cascade to the Kolmogorov scale. A simple mathematical model incorporating these ideas is presented. This model predicts a Reynolds number dependence for the nitric oxide formation rate that is in good agreement with measurements in both methane and hydrogen jets burning in air. These mathematical model concepts have been incorporated into a simplified computer program capable of treating the detailed chemical kinetics of a gas flame. The model has been used to predict NO formation in H_2/air and CH_4/air flames and results compare favorably with experimental data.

TABLE OF CONTENTS

Section	Page
Abstract	iii
List of Figures	vi
List of Tables	vii
Acknowledgements	viii
1.0 Introduction	1-1
PART I - THEORETICAL DEVELOPMENT (J.E. Broadwell)	I-1
I.1 Jet Mixing and Flame Length	I-1
I.2 The Jet Structure	I-9
I.3 The Treatment of Slow Chemical Reactions: Nitric Oxide Generation in Fuel Jets in Air	1-10
PART II - NUMERICAL ANALYSIS (T.J. Tyson, C.J. Kau, J.E. Broadwell)	II-1
II.1 Introduction	II-1
II.2 Model Development	II-1
II.3 Numerical Procedures and Heat Transfer Model	II-12
II.4 Sample Calculation and Sensitivity of Model Parameters	II-13
II.5 Comparison with Experimental Data and Discussion of Results	II-15
II.6 Concluding Remarks	II-24
References	II-26

LIST OF FIGURES

Figure		Page
1-1	Effect of Normality Ratio and Reynolds Number on Liquid Visual Jet Length	I-2
1-2	Effect of Normality Ratio on Visual Liquid Jet Length for Nozzles of Various Shapes	I-4
1-3	Sketch of Turbulent Jet Entrainment	I-5
1-4	Dependence of Turbulent Flame Length on $(\rho_o/\rho_a)^{1/2}\phi$	I-8
1-5	Instantaneous Temperature Profiles Across a Two-Dimensional Heated Jet at x/D = 4.5	I-11
1-6	Sketch of Turbulent Jet Reaction Model	I-13
2-1	Sketch of Turbulent Jet Entrainment	II-3
2-2	Flame Length vs. $\left(\frac{\dot{m}_t}{\dot{m}_o}\right)_{st}\sqrt{\frac{\rho_o}{\rho_m}}$	II-5
2-3	Schematic of Reactor Model	II-10
2-4	Sensitivity of $\beta(\alpha = 0.7)$	II-14
2-5	Sensitivity of Radiative Heat Transfer Parameter $\alpha(\beta = 10)$	II-16
2-6	Effect of Radiative Heat Transfer on Flame Core Temperature History	II-17
2-7	Comparison of Model Calculated NO vs. Measurements ($Fr = 6 \times 10^{-5}$) for H_2/Air Flames	II-18
2-8	Predicted E/τ_o versus Re_o for H_2/Still Air Flames (at Constant Froude No., $Fr = 6 \times 10^5$)	II-19
2-9	Overall NO Formation in Flame-sheet Zone and Overall NO Destruction in Flame-core Zone	II-21
2-10	Emission Index versus Re_o (H_2/Air Flame)	II-23

LIST OF TABLES

Table		Page
2-1	Flame Length Data	II-6
2-2	Comparison of Predicted and Measured Emission Indices ... for CH_4/Air Turbulent Diffusion Flame	II-25

ACKNOWLEDGEMENTS

The authors are pleased to acknowledge the contributions of many discussions with Frank Marble to the development of the ideas reported here. One of the authors (J.E.B.) is grateful to his colleagues of the Fluid Mechanics Group at the California Institute of Technology for generously sharing their new insights into turbulent flows. The early experimental investigation of jet structure by Paul Dimotakis was especially valuable. Special thanks are also due to R.E. Breidenthal who was an unofficial collaborator.

1.0 INTRODUCTION

One of the central focuses of EPA's combustion research program has been development of combustion control technologies to limit formation of nitrogen oxides (NO_x) from fossil fuel fired flames. The Fundamental Combustion Research (FCR) program has served to help advance understanding of critical combustion processes controlling NO_x formation. The present study was conducted to develop an improved understanding of the coupling between fundamental fluid mechanics and chemical processes in turbulent diffusion flame. Specifically, the study focused on one of the simplest flow configurations: a jet of methane fuel discharging into ambient air.

Many practical stationary combustion processes use diffusion type flames where the combustion rate is controlled by mixing of fuel and air. A typical characteristic of low NO_x burners for pulverized coal fired utility boilers is that the fuel/air mixing rates are retarded providing an elongated flame. The present FCR project does not address the practical problems associated with utility boiler burners but instead focuses on better understanding the critical fuel/air mixing process in flames.

Classical fluid mechanics provides the view of turbulent flow as an enhancement to the viscous processes where, for example, mixing rates are describable through the product of a mean velocity gradient and a "turbulent" diffusivity. Similarly, shear stress could be described by the product of mean velocity gradients and a "turbulent" viscosity. These classical flow theory notions have been extremely effective in describing bulk flow processes such as flow of fluid through pipes or over aircraft wings. Recent experiments and turbulent theory developments (see for example Brown and Roshko, 1974 and Roshko, 1977) are leading to a new view of the basic processes involved in turbulent shear flow. This new view has evolved from recognition of the existence and importance of large-scale organized structure in turbulent shear flows. The large-scale structures are seen to engulf fluid from either side and distribute it across the layer. The mixing of fluids on a molecular scale occurs at the interface formed between alternating layers of jet and reservoir fluid. If these alternating layers represent fuel and oxidizer, the local combustion environment is radically different than would be predicted by classical turbulent mixing theories.

The current FCR study was conducted in two parallel parts and the report is also organized in that way. In Part I, a mathematical model has been developed while in Part II, this model is extended and adapted to a computer simulation. Both parts of the study and report make comparison of predictions with available experimental results.

PART I THEORETICAL DEVELOPMENT (J.E. Broadwell)

I.1 Jet Mixing and Flame Length

Information providing important insights into turbulent mixing process is available from a variety of sources including a particularly significant study by Weddell (1941). A major review of the early turbulent flame studies is provided by Hottel (1953) in the Fourth Combustion Symposium. Hottel's review covers the work of Weddell, who studied liquid jets consisting of an alkali solution marked with phenophthalein discharging into an acid reservoir. The jet, which is initially red, becomes colorless when it entrains and mixes with sufficient acid. Weddell states that the flow strikingly resembles a turbulent flame. In the experiments, the reservoir-jet normality ratio was varied between two and ten. This ratio, R, is the mass of reservoir fluid required to cause the color to vanish from a unit mass of jet fluid when the two are mixed homogeneously. For fixed values of R, the distance, L, over which the color was visible was interpreted as "flame length" and presented by Hottel as a function of jet Reynolds number, Re_o. Figure 1-1 is replotted from Hottel's paper.* Here $Re_o = \rho U_o d_o/\mu$, where d_o and U_o are the initial jet diameter and velocity respectively, ρ the density and μ the viscosity.

One of the noteworthy features in Figure 1-1 is that at sufficiently high Reynolds number the flame length, measured in jet diameters, becomes independent of Reynolds number. An explanation for this observation was proposed some time ago by Broadwell (see Witte et. al.,1974). When the marked jet disappears <u>every</u> element of jet fluid has molecularly mixed with at least R parts of reservoir fluid. The required reservoir fluid is entrained into the jet at some upstream location. Subsequent mixing of the jet and reservoir fluids occurs by intertwining on an ever decreasing scale--cascade--to the Kolmogorov scale λ_o. These intertwining motions are <u>inviscid</u> and reach λ_o after time, τ_d, which is proportional to the local macroscale parameters, jet diameter and velocity. That is, $\tau_d \sim d/u$. The Kolmogorov scale λ_o is also related to the jet velocity and viscosity by the expressions

---

* In the original figure, the flame length is measured from the jet "breakpoint," the station at which the jet begins to spread linearly. This point is a few diameters from the nozzle exit at high reynolds number and thus for current purposes may be measured from the exit.

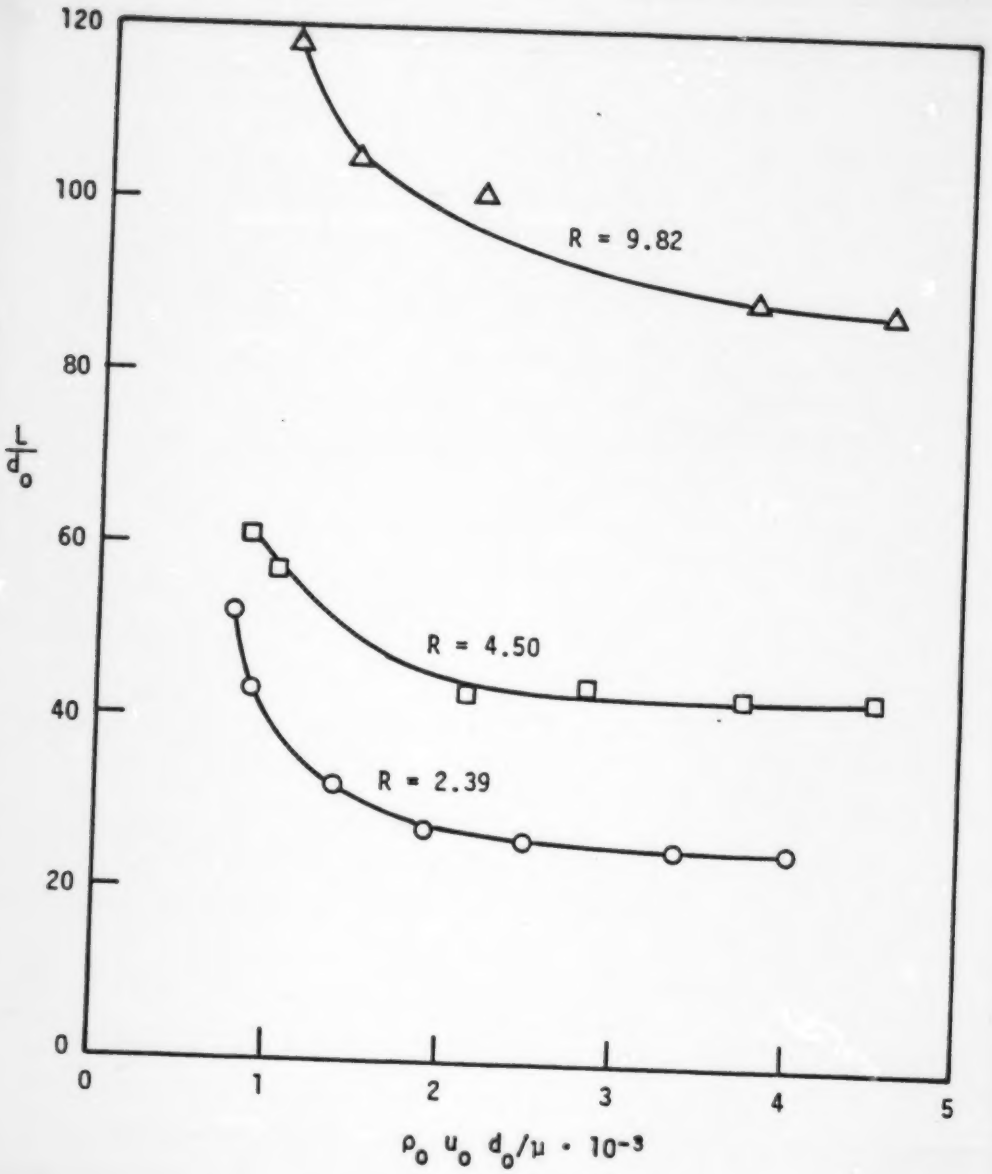

Figure 1-1.
Effect of Normality Ratio and Reynolds Number on Liquid Visual Jet Length, from Hottel (1953).

$$\lambda_o \sim (\nu^3/\varepsilon)^{1/4} \sim (\nu^3 d/u^3)^{1/4}$$

where ν is the kinematic viscosity, μ/ρ, and ε is the kinetic energy dissipation rate $\sim u^3/d$ (see, for instance, Tennekes and Lumley, 1972). The time for diffusion to occur across this micro scale, τ_λ, is given by

$$\tau_\lambda \sim \lambda_o/D \sim Sc/Re_d^{1/2}\ (d/u), \qquad (1)$$

where D is the molecular diffusion coefficient, Sc is the Schmidt number ($\mu/\rho D$), and $Re_d = \rho ud/\mu$. Therefore, the ratio, T, of the diffusion time to the large scale break-down time is

$$T \sim \tau_\lambda/\tau_d \sim Sc/Re_d^{1/2} = Se/Re_o^{1/2} \qquad (2)$$

since jet Reynolds number does not vary with axial distance, x.

Equation (2) above can be used to explain the observations from Figure 1-1. The equation shows that at high Reynolds number the diffusion time is short compared to the entrainment-breakdown time and consequently the mixing time is limited by the slower, Reynolds number independent process. Stated another way, negligible additional distance is required for molecular mixing to be completed after the jet and reservoir fluids have intertwined and cascaded to λ_o. Finally, when the chemical reaction rate is fast relative to the diffusion rate (as it is in the phenophthalein reaction), the "flame length" will also be independent of Re_o. Equation (2) also predicts that for high Reynolds number the flame length is independent of Schmidt number. Evidence on this point is discussed later.

Weddell combined the high Reynolds number data in Figure 1-1 with data for nozzles of other size and shape and presented it in the form of Figure 1-2 to show that "flame length" varies almost linearly with normality ratio, R. The argument developed above for Reynolds number independence explains this result as well. Figure 1-3 is a sketch of a circular jet schematically indicating entrainment, which is a constant value per unit length. The jet in Weddell's experiments disappears when every element of jet fluid is molecularly mixed with R units of reservoir fluid. In Figure 1-3, suppose that reservoir fluid enters the jet between the origin and x_o and that

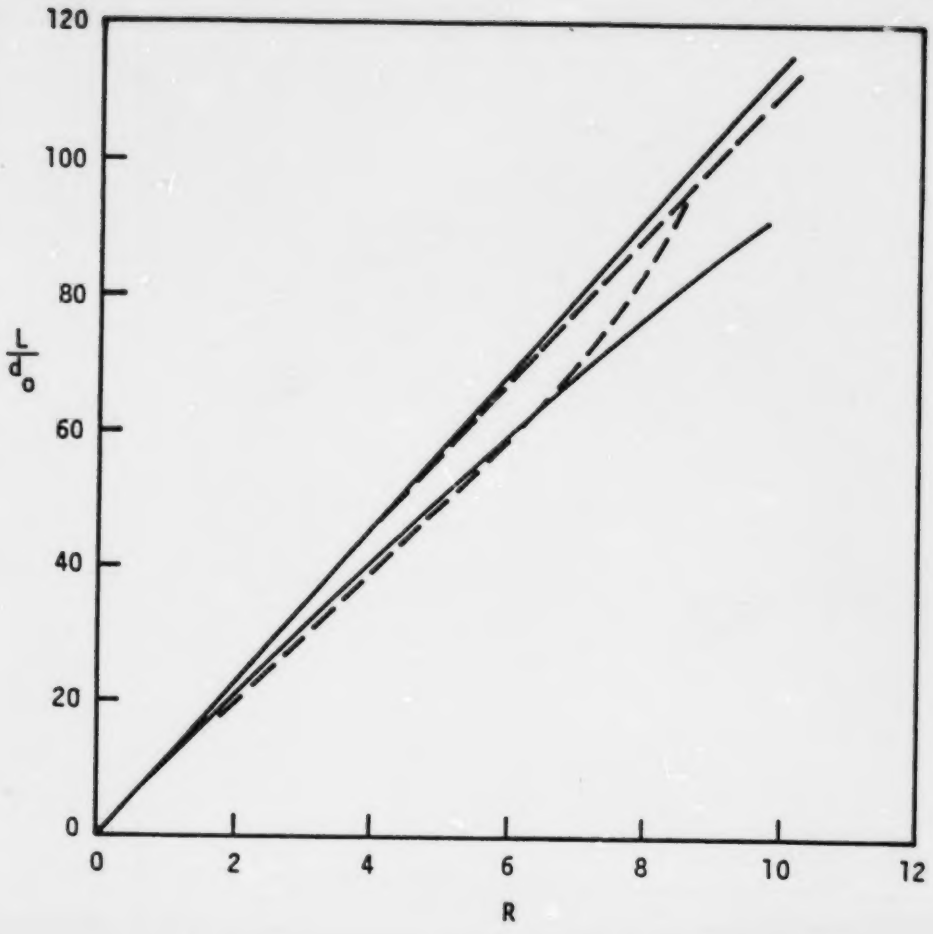

Figure 1-2.
Effect of Normality Ratio on Visual Liquid Jet Length for Nozzles of Various Shapes from Hottel (1953).

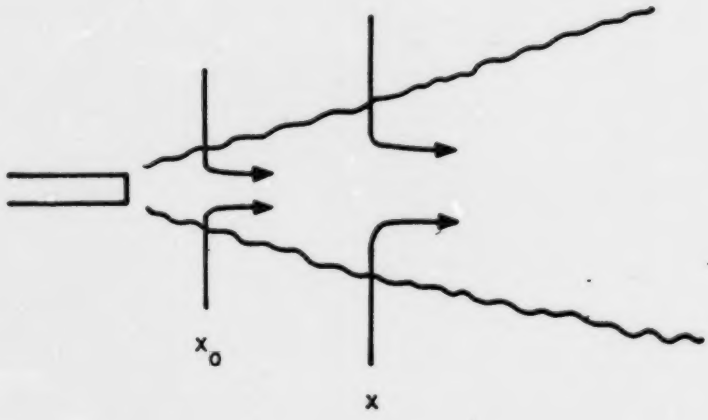

Figure 1-3. Sketch of Turbulent Jet Entrainment.

molecular mixing is complete at x. Since the quantity of entrained fluid rises linearly, the amount molecularly mixed will also increase linearly, at a slower rate, if x is linear with x_o. That this is so follows immediately from the above discussion: since the breakdown time is proportioned to d/u, the required distance is proportional to d and hence to x_o. Then since negligible additional distance is needed for the molecular mixing, the flame length varies linearly with R.

Hottel (1953) also reviewed the flame length data for various gaseous fuel jets in air and compared it with the theoretical work of Hawthorne, Weddell, and Hottel (1949) and others. The above analysis may be applied to these jets if the difference in fuel and air density and the effect of heat release on density can be accounted for. An approach to accounting for these effects is outlined next.

For current purposes, attention will be restricted to the high Reynold's number jets and to situations where the buoyancy force is small compared with the jet momentum. Initial consideration will be given to non-reacting jets whose density differs from that of air (the reservoir fluid). Ricou and Spalding (1961) examined this case experimentally and found that, at sufficiently high Reynolds number, entrainment is independent of Reynolds number and is linear with axial distance, x. Their experiments show also that the effect of the jet-air density difference on entrainment can be expressed in the form

$$m_t/m_o = c_1(\rho_a/\rho_o)^{1/2}\ x/d_o, \qquad (3)$$

in which m_t and m_o are the total and initial jet mass flow respectively, ρ_a and ρ_o are the air and fuel density and c_1 is a constant equal to 0.32. The authors point out that the form of equation (3) confirms a result form dimensional analysis that the entrainment is determined by the jet momentum (see Section II.2 in the current report). For the current study a similar argument is made that, as an approximation at least, the form of equation (3) would also apply when there is reaction between the fuel jet and air. The previous analysis of chemically reacting liquid jets can be combined with the entrainment estimate of equation (3) to develop a prediction of the flame length for gas fuels in air.

First it should be noted that equation (3) is applicable only when x/d_o is large and the entrained air flow is correspondingly large relative to the fuel flow, m_o. Then m_t is approximately the air flow rate, m_a. The fuel will be completely consumed at the axial station where a stoichiometric amount of air has been molecularly mixed with every element of fuel. The argument given above that the molecular mixing rate is controlled by the entrainment rate allows m_t/m_o in equation (3) to be set equal to the air-fuel stoichiometric ratio, ϕ, and leads to the prediction that flame length, L, will vary according to

$$L/d_o = (1/c_2)\ (\rho_o/\rho_a)^{1/2}\phi, \qquad (4)$$

in which c_2 is a new constant (which will be smaller than c_1). As before the fuel-air reaction rate is assumed to be rapid relative to mixing.

Hottel (1953) collected flame length data for several fuels (hence different values of ϕ). These data are presented in Figure 1-4 and are seen to be approximately linear with $(\rho_o/\rho_a)^{1/2}\phi$ in accord with equation (4). Also shown in Figure 1-4 is the average "flame length" data for liquid jets given earlier in Figure 1-2. Note that the normality ration R in Weddell's experiments has the same effective meaning as ϕ. The previous analysis leading to equation (2) had led to the prediction that at high Reynolds number flame length should be independent of Schmidt number. This is confirmed in Figure 1-4 where little difference is seen between liquid and gaseous "flame length" even though the Schmidt number ratio is approximately 1000.

Hottel makes no direct comparison between the liquid and gaseous results but presents a correlation of the fuel data with the analysis of Hawthorne, Weddell, and Hottel (1949). In that analysis, the flame length is correlated with the jet width at which the stoichiometric amount of air is entrained. The jet spread angle is assumed constant and equal for all fuels, and chemical reactions are assumed to occur simultaneously with entrainment. The resulting equation for flame length is

$$\frac{L - s}{d_o} = 5.3\ (\phi + 1)\ \frac{T_f}{\alpha\ T_o}\ \frac{1}{(\phi + 1)} + \frac{\phi}{(\phi + 1)}\ \frac{M_a}{M_o}^{1/2}$$

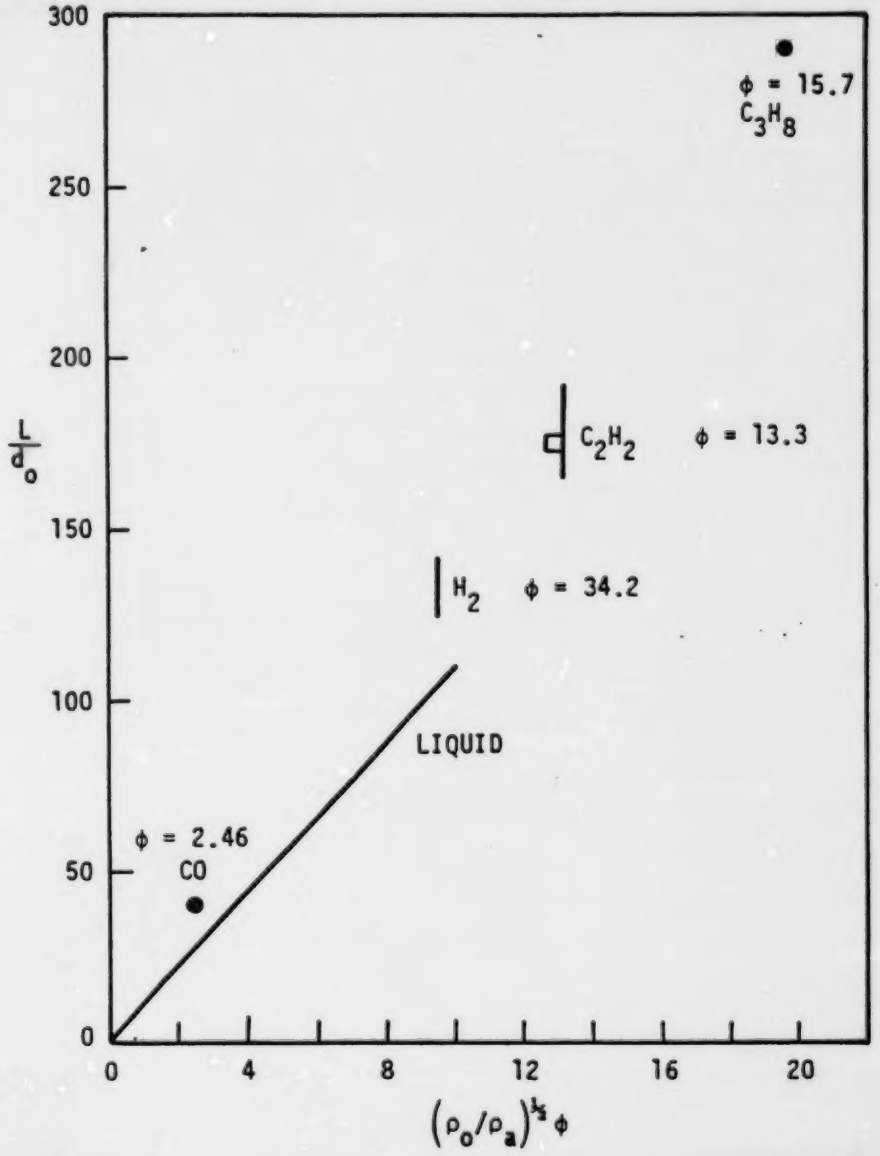

Figure 1-4.
Dependence of Turbulent Flame Length on $(\rho_o/\rho_a)^{1/2}\phi$.
Data from Hottel (1953).

where T_f if the adiabatic combustion temperature of a stoichiometric mixture, T_o the nozzle gas temperature, α the moles of reactants per mole of products in a stoichiometric mixture, M_a and M_o are the molecular weights of air and nozzle gas respectively, and s the distance to the jet break point. It is seen that for ϕ large compared to unity and with the assumption the T_f and α do not vary widely, this expression reduces in form to that derived above. That the two analyses should be in approximate agreement is not surprising once it has been established that molecular mixing rate is linear in axial distance as is the entrainment.

Before summarizing the above results, it is important to clarify an aspect of the mixing process that has not been discussed. Following the entrainment of a particular volume of reservoir fluid into the jet and during the subsequent cascade in scales to the Kolmogorov scale, λ_o, molecular diffusion is occurring at the interface between the two fluids. Hence some molecular mixing takes place before λ_o is reached. The end of the flame, however, is reached when every part of the jet fluid mixes with the required amount from the reservoir. Thus τ_λ in equation (1) is the time required for the completion of mixing after the Kolmogorov scale is reached.

The analysis developed above, with its satisfactory agreement with experiment, may be summarized as follows. In both gaseous and liquid jets at sufficiently high Reynolds number, the distance needed to mix, at the molecular level, a given amount of reservoir fluid with the jet fluid is independent of Reynolds number. The length is determined by the large scale entrainment rate. The "flame lengths" for gases and liquids are, therefore, approximately the same, i.e., the flame length is independent of Schmidt number. Finally the flame length depends linearly on the parameter $(\rho_o/\rho_a)^{1/2}\phi$, a consequence of the assumption that the jet entrainment rate is determined solely by the jet momentum.

I.2 The Jet Structure

The picture of the mixing process in jets that was developed in the preceding section emerged in an attempt to understand the data in Figure 1-4. The emphasis in that section was on the dependence of mixing on the various parameters. However, the magnitude of the mixing rate implied by the data,

together with the parameter dependence has further significance. Note from Figure 1-2 that at 20 diameters from the nozzle exit, for instance, every element of jet fluid is mixed with at least two parts from the reservoir. Hence large quantities of the entrained fluid reach the jet center near the nozzle exit. This fact, viewed in the light of recent photographic evidence obtained by P.E. Dimotakis (1981), suggests that reservoir fluid is carried into the jet in large scale coherent structures and that the breakdown to small scales begins from this initial state. A natural idealization of these processes is that there is no radial variation of the reservoir-jet mixture ratio in the mixed fluid. In this view, the usual bell-shaped mean concentration profiles arise only from a radial variation in the ratio of mixed fluid to pure reservoir fluid.

For two-dimensional jets, the measurement of Uberoi and Singh (1975) provide strong support for this picture. They projected hot wires across a slightly heated jet to obtain virtually instantaneous temperature distributions, examples of which are given in Figure 1-5. Within the jet there is seen to be little lateral temperature variation. These authors interpret their results to mean the lateral position of the jet is fluctuating and show that a superposition of the instantaneous profiles yields the well-known bell-shaped curves.

The inference to be drawn from these data and from the discussion in Section I.1 is that mixing in turbulent jets does not occur through a gradient diffusion process. Instead the two fluids intermix uniformly on a large scale and reach a molecularly mixed state as has already been described. The same view of mixing in shear layers has been put forward by Broadwell and Breidenthal (1981).

I.3 The Treatment of Slow Chemical Reactions: Nitric Oxide Generation in Fuel Jets in Air

The first step in developing a model framework for treating nitric oxide generation in jet is recognition that the mixing rate inferred from Figure 1-4 applies regardless of chemical reactions that may take place. That is, for example, in the case of a fuel of stoichiometric ratio, ϕ, equal to ten and flame length 100 d_o, all the fuel elements are mixed at upstream stations with either air or partial combustion products at a linear rate. This mixing occurs at a rate, of course, such that the flame would have ended at 20 d_o had

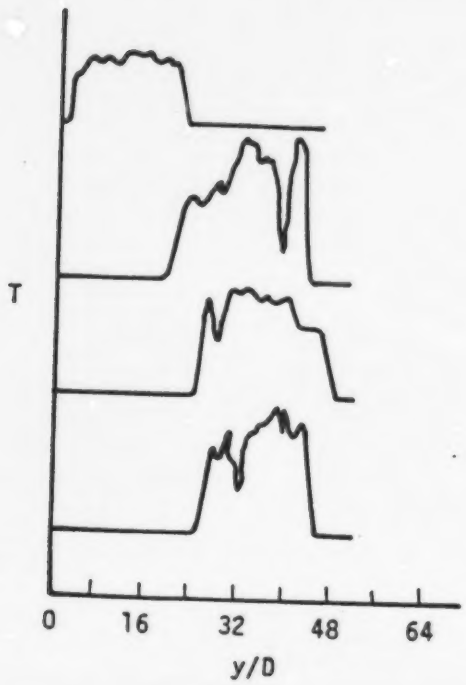

Figure 1-5.
Instantaneous Temperature Profiles Across a Two-Dimensional Heated Jet at x/D = 45. Mean Velocity Axis 0.305 CM/SEC. From Uberoi and Singh (1975).

ϕ been equal to two. The basis for this assertion is that a difference in molecular diffusion coefficients between reactants and products have no influence on the mixing rate. An explicit expression for the air addition rate will be given later.

The analysis and discussion to this point has dealt with situations in which the chemical reaction rates are fast relative to mixing, and in which, therefore the reaction rate is controlled by the entrainment rate. This approximation is appropriate for the energy releasing reactions in fuel jets but may not be appropriate for the slower reactions which generate nitric oxide by thermal fixation. The inclusion of these reactions, therefore, necessitates a refinement in the model.

In the model as formulated so far, the fast reactions take place in the molecular diffusion zones-strained laminar flames (see Marbel and Broadwell 1977, 1980)-during the cascade to the Kolmogorov scale, λ_o, and as the mixture is homogenized by diffusion at this scale. In both situations the fuel and oxidizer react at the stoichiometric ratio. The slow reactions occur during these processes as well but continue, at rates set by the chemical kinetics, after the mixture has been homogenized.

These ideas can best be described in Lagrangian frame, i.e., by following a unit mass of fuel after it leaves the nozzle and mixes with air at the known rate.

At any given time, the fuel mass and the air entrained up to that time are undergoing the cascade to λ_o or have reached this scale. It will be argued later in this report that the nature of the cascade is such that relatively little flame is generated until just before λ_o is attained and the mixture is homogenized. If this is the case, the reactions in these two processes may, as an approximation, be treated together and the time that the reactants remain at the stoichoimetric ratio is limited by the diffusion time τ_λ, derived in Section I.1.

The model is conveniently described with the help of the sketch in Figure 1-6. The reactors A and B together contain a unit mass of fuel to which air is added at the rate m_a. The reactions that occur at stoichiometric conditions take place in reactor B; slow reactions proceed in both A and B.

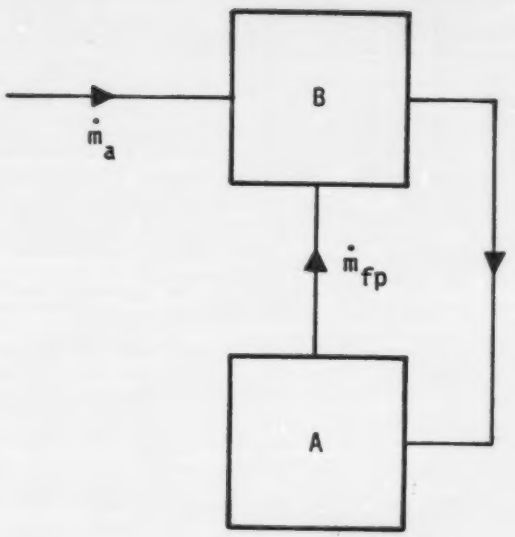

Figure 1-6. Sketch of Turbulent Jet Reaction Model.

It is assumed, as a tentative approximation, that the salient feature of the reactions in B is that they occur at stoichiometric conditions and that the details of the strained flame structure and of the homogenizing diffusion process are unimportant. A natural implementation of this approximation would be to take reactor B to be a well-stirred chemical reactor and reactor A as plug flow reactor. This concept will be developed in more detail in Part II of this report. However, it should be noted that a well-stirred reactor with appropriate residence time is a close simulation of the reaction zone of a strained flame.

As implied above, a critical parameter in the model is the residence time in reactor B, τ_b. Analysis presented earlier argues that this would be τ_λ if most of the flame sheet were generated just before the scale of concentration variation were reduced to λ_o. A detailed examination of the nature of the buildup in time of flame sheet between a given quantity of entrained air and the fuel-product mixture indicates that this may be so. The approach was formulated by R.E. Breidenthal (see Broadwell and Breidenthal 1981) for this process in turbulent shear layers, and modified by V.A. Kulkarny (private communication).

The idea is that the interface surface, S, per unit volume, being inversely proportional to the scale of the distortions, λ, caused by the turbulence can be estimated from the scale variation with time. It is assumed that the Kolmogorov description of the cascade in scales applies to the jet mixing, at least at the small scales. The procedure is as follows.

The basic concept [see, for instance, Landau and Lifshitz (1959)] is that for scales down to λ_o, the motion is inviscid and the kinetic energy flux, e, is, constant, i.e., that

$$e \sim v_\lambda^3/\lambda \sim u^3/d \text{ for } \lambda_o < \lambda < d.$$

This statement alone is not sufficient to determine the dependence of λ on the time, t, and further progress must rely solely on dimensional arguments. To quote Landau and Lifshitz "v_λ may also be regarded as the velocity of turbulent eddies of size λ." Thus if it is assumed that in one "turn over time" the eddy gives up a large fraction of its energy, the time spent at λ_1 is

$$\Delta t \sim \lambda_1/v_1 \sim \lambda_1/e^{1/3}\,\lambda^{1/3} \sim \lambda_1^{2/3}/e^{1/3}.$$

Now a further decision is required concerning the new scale generated. V.A. Kulkarny argues that, because the process is self similar, the change in scale should be scaled with λ and thus the memory of the initial scale lost. Therefore

$$dt \sim \frac{\kappa_1 \lambda^{2/3}}{e^{1/3}} \frac{d\lambda}{\lambda}, \qquad (5)$$

where κ_1 is a constant.* Integration of equation (5) and use of the expression for e give an estimate for the time to reach a given scale λ, starting at scale d,

$$t(\lambda) = \kappa_2\, d/u \left[1 - (\lambda/d)^{2/3}\right]$$

and since $\lambda_o = \kappa_3\, d/Re_o^{3/4}$, the time τ_d to reach λ_o is

$$\tau_d = k_2\, d/u \left(1 - k_3/Re_o^{1/2}\right) = k_2\, d/u, \text{ for } Re_o \gg 1$$

where κ's are constants. Thus in accord with the discussion in Section I.1, at high Re_o the time to reach λ_o is independent of Re_o. With $S \sim 1/\lambda$ the growth in flame sheet area per unit volume can be expressed as

$$S \sim 1/d \left(1 - t/\tau_d\right)^{-3/2},$$

which shows the anticipated rapid increase in S when t near τ_d.

Since the diffusion at λ_o follows immediately, it is reasonable to assume that the fuel and oxidizer are mixed stoichiometrically only for the time required by the diffusion process, $\tau_\lambda \sim \tau_d/Re_o^{1/2}$ (when the Schmidt number

---

* Here, for convenience, a continuous change in scale is assumed. The actual situation may better be described by jumps between discreet scales, but only qualitative results are required at this stage of model development.

is unity). Thus the residence time in reactor B, τ_b, is taken proportional to $(d/u)Re_o^{-1/2}$. If radiation is neglected, the mixture is at the adiabatic glame temperature for this length of time also. Since the nitric oxide producing reaction rates depend strongly on temperature it would appear to follow immediately that the nitric oxide level would scale with $(d/u)Re_o^{-1/2}$. It is premature to draw this conclusion for two reasons:

1) As is shown in Part II, radiation, in some experiments at least, has a significant influence, and

2) Near the end of the flame, the entire fuel mixture (i.e., in both reactors A and B) reaches the stoichiometric condition.

These efforts are addressed in the numerical modeling portion of the current study presented in Part II.

PART II NUMERICAL ANALYSIS (T.J. Tyson, C.J. Kau, J.E. Broadwell)

II.1 Introduction

This second part of the report develops a detailed numerical model of a simple gaseous turbulent diffusion flame with associated nitric oxide formation. The basic underlying concepts of the model were presented in Part I and are summarized as follows:

- Macroscopic entrainment of a turbulent jet is independent of Reynolds number and is linearly proportional to the axial (mainflow direction) distance.
- The macroscopically entrained fluid is mixed uniformly with the jet fluid so that there is no macroscopic variation in radial direction.
- The macroscopically entrained fluid is engulfed into the jet in large coherent structures; subsequently, breakdown to small scale structures is through inviscid, instable motion.
- The majority of the interface surfaces are generated just before the structures reach the Kolmogorov scale.
- Combustion takes place in the interface surfaces (or flame sheets) stoichiometrically at the Kolmogorov scale, and the interface surfaces are homogenized by molecular diffusion at this scale.

The mathematical model postulated here consists of simple chemical reactors arranged in a manner to account for the basic features listed above as well as the detailed chemical kinetics of combustion reactions and NO formation. A simple flame radiation model in incorporated to account for radiative energy loose which can have a strong impact on temperature and NO formation.

II.2 Model Development

In this section, the differential equation describing the proposed model are put in a form suitable for numerical computations. The basic turbulent

jet mixing/reaction model developed in Part I will be partially redeveloped to assist in empirically evaluating critical model constants. The basic flow configuration to be modeled is a circular jet of fuel issuing into a reservoir of stationary air.

For the basic flow condition being modeled, the conservation of momentum flux requires that

$$J = \frac{\pi}{4} \rho_m U_m^2 d_m^2 = \pi \rho_o U_o d_o^2$$

where subscripts "m" and "o" refer to the local mean and initial jet properties respectively and all other terms are as defined earlier in Part I. The configuration is illustrated in Figure 2-1. The above equation can be rearranged to provide an expression for the local mean main flow velocity U_m in terms of initial density ρ_o and initial velocity U_o by:

$$U_m = \left(\frac{\rho_o}{\rho_m}\right)^{1/2} \left(\frac{U_o d_o}{d_m}\right) \qquad (6)$$

By definition, the local mass flux per unit initial jet mass flux can be written as

$$\left(\frac{\dot{m}_l}{\dot{m}_o}\right) = \frac{\rho_m U_m d_m^2}{\rho_o U_o d_o^2}$$

Eliminating U_m from the above equation by using Eqn. (6) gives

$$\left(\frac{\dot{m}_l}{\dot{m}_o}\right) = \left(\frac{\rho_m}{\rho_o}\right)^{\frac{1}{2}} \left(\frac{d_m}{d_o}\right) \qquad (7)$$

As in Part I, the jet spreads linearly at approximately a constant angle, except for within a few diameters from the nozzle exit and is independent of the type of jet fluid and physical conditions. The jet radius is in linear proportion to the axial distance, i.e.,

$$d_m = 2k_2 X \qquad (8)$$

where k_2 is the tangent of half jet angle.

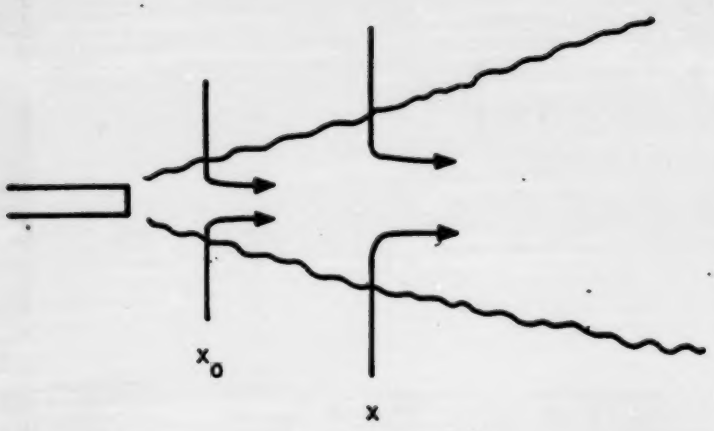

Figure 2-1. Sketch of Turbulent Jet Entrainment.

Substituting Eqn. (8) into Eqn. (7) becomes:

$$\left(\frac{\dot{m}_t}{\dot{m}_o}\right) = 2k_2 \sqrt{\frac{\rho_m}{\rho_o}} \left(\frac{X}{d_o}\right) \qquad (9)$$

The turbulent entrainment law derived by Ricou and Spalding (1961) recommended $k_2 = 0.16$. [C_1 from equation (3) equals 2 times k_2.] The axial distance where turbulent-jet-entrained stoichiometric amount of air can be evaluated from Eqn. (9) by simply setting (m_t/m_o) to be stoichiometric ratio, i.e.:

$$\frac{L_{macro}}{d_o} = \frac{1}{2k_2} \left(\frac{\dot{m}_t}{\dot{m}_o}\right)_{st} \sqrt{\frac{\rho_o}{\rho_m}} \qquad (10)$$

Flame length is the indication of the axial distance where the stoichiometric amount of air is microscopically mixed with the fuel when combustion reactions are fast and when combustion is also mixing controlled. The flame length data for various gaseous fuel jets in air from the classic work of Hawthorne, Weddell and Hottel (1949) and the recent work of Bilger and Beck (1974) and Peter and Donnerback (1981) are plotted in Figure 2-2. The physical parameters of these flames are also given in Table 2-1. Experimentally, the flame length here is referred to as the analytical flame length which represents the axial distance of the point where 99 percent of the combustion is completed (based on sample gas). As can be seen from Figure 2-2, almost all the points fall on a straight line which has a slope of 9.217. The lengths [Eqn. (10) ~ $K_2 = 0.16$] of the macroscopic entrainment of stoichiometric amount of air for various flames are also plotted as the solid line in Figure 2-1. The plot suggests a linear proportionality of flame length to

$$\left(\frac{\dot{m}_t}{\dot{m}_o}\right)_{St} \sqrt{\frac{\rho_o}{\rho_m}}$$

and a constant ratio of the microscopic mixing rate to the macroscopic entrainment rate, i.e.,

$$(\dot{m}_t)_{micro} = k_1 (\dot{m}_t)_{macro}$$

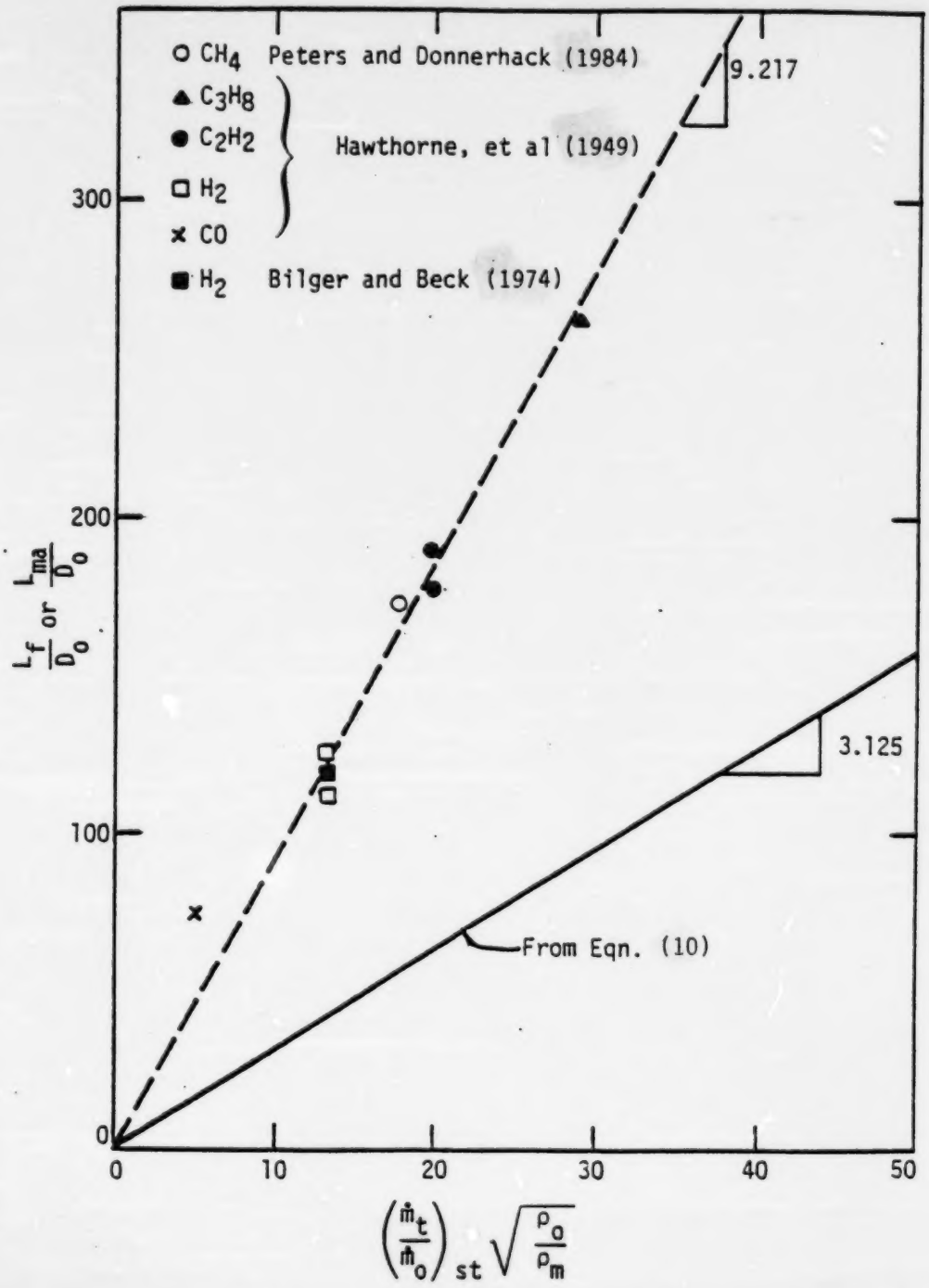

Figure 2-2. Flame Length vs. $\left(\frac{\dot{m}_t}{\dot{m}_o}\right)_{st}\sqrt{\frac{\rho_o}{\rho_m}}$

Table 2-1. Flame Length Data.

Data No.	Fuel Composition	d_o (cm)	$\frac{\rho_a}{\rho_o}$	$\frac{\rho_o}{\rho_m}$*	$\left(\frac{\dot{m}_t}{\dot{m}_o}\right)_{st}$	Re_o**	Fr***	$\left(\frac{\dot{m}_t}{\dot{m}_o}\right)_{st}\sqrt{\frac{\rho_o}{\rho_m}}$	L_f/D	L_{ma}/D****	Source
1	Hydrogen H_2	0.476	14.45	0.138	35.047	2870	92,000	13.02	114	40.68	Hawthorne et al (1949)
2	Hydrogen H_2	0.462	14.45	0.138	35.047	3580	158,000	13.02	126	40.68	Hawthorne et al (1949)
3	Propane C_3H_8	0.3175	0.67	2.985	16.7	29,000	54,000	28.85	263	90.16	Hawthorne et al (1949)
4	Acetylene C_2H_2	0.3175	1.036	1.930	14.2	17,400	88,000	19.72	176	61.70	Hawthorne et al (1949)
5	Acetylene C_2H_2	0.3175	1.034	1.934	14.2	32,400	307,000	19.74	188	61.70	Hawthorne et al (1949)
6	CO	0.635	1.034	1.934	3.45	5,090	2,415	4.79	75.6	14.99	Hawthorne et al (1949)
7	Hydrogen H_2	0.635	14.45	0.138	35.047	12,270	60,000	13.02	120	40.68	Bilger & Beck (1974)
8	CH_4	0.30	1.80	1.11	17.20	3,200	14,710	18.12	170	56.63	Peters et al (1984)

* $\rho_m \approx 0.5\ \rho_a$ ** Reynolds No. = $U_o d_o/\nu_o$ *** Froude No. = U_o^2/gd_o **** From Eqn. (10)

Numerically, Figure 2-1 gives the proportional constant, k_1, a value of 0.339; that is to say, the microscopic mixing rate is approximately one-third of the macroscopic entrainment rate. By replacing the macroscopic entrainment rate in Eqn. (10) with the above relation, the expression for dimensionless flame length becomes:

$$\frac{L_f}{d_o} = \frac{1}{2k_1k_2}\left(\frac{\dot{m}_f}{\dot{m}_o}\right)_{st}\sqrt{\frac{\rho_o}{\rho_m}} \qquad (11)$$

The logical extension of the above conclusion is that "the microscopic mixing rate in linearly proportional to $\sqrt{\frac{\rho_o}{\rho_m}}\left(\frac{X}{d_o}\right)$"; i.e.,

$$\left(\frac{\dot{m}_f}{\dot{m}_o}\right)_{micro} = k_3\sqrt{\frac{\rho_o}{\rho_m}}\left(\frac{X}{d_o}\right) \qquad (12)$$

where $k_3 = 2k_1k_2 = 0.1085$.

The definition of velocity from Eqn. (6) gives

$$U_m = \frac{dX}{dt} = \sqrt{\frac{\rho_o}{\rho_m}}\frac{U_o d_o}{2k_2 X} \qquad (13)$$

Carrying out the integration of the above equation with respect to time by assuming a constant mean density, ρ_m, results in the following space-time relation:

$$\frac{X}{d_o} = \left(\frac{\rho_o}{\rho_m}\right)^{1/4}\left(\frac{U_o t}{k_2 d_o}\right)^{1/2} \qquad (14)$$

Substituting Eqn. (14) into Eqn. (12) results in an expression for microscopic mixing in terms of time:

$$\left(\frac{\dot{m}_t}{\dot{m}_o}\right)_{micro} = k_3 \left(\frac{\rho_o}{\rho_m}\right)^{1/4} \left(\frac{U_o\, t}{k_2 d_o}\right)^{1/2} \qquad (15)$$

The time derivative of the above equation gives the microscopic air mixing rate per unit of initial fuel flux as:

$$\frac{d}{dt}\left(\frac{\dot{m}_a}{\dot{m}_o}\right)_{micro} = \frac{d}{dt}\left(\frac{\dot{m}_t}{\dot{m}_o} - 1\right) = \frac{d}{dt}\left(\frac{\dot{m}_t}{\dot{m}_o}\right) = \frac{k_3}{2}\left(\frac{\rho_o}{\rho_m}\right)^{1/4} \left(\frac{U_o}{k_2 d_o t}\right)^{1/2} \qquad (16)$$

The microscopic fuel mixing rate is

$$\frac{d}{dt}\left(\frac{\dot{m}_f}{\dot{m}_o}\right)_{micro} = \frac{1}{\Phi}\frac{k_3}{2}\left(\frac{\rho_o}{\rho_m}\right)^{1/4} \left(\frac{U_o}{k_2 d_o t}\right)^{1/2} \qquad (17)$$

where ϕ is the air fuel mass ratio of the microscopic mixture. The overall unburned raw fuel left in the flame per unit of initial raw fuel flux is evaluated by

$$1.0 - \frac{1}{\Phi}\left(\frac{\dot{m}_t}{\dot{m}_o}\right)_{micro}$$

or, explicitly

$$1.0 - \frac{k_3}{\Phi}\left(\frac{\rho_o}{\rho_m}\right)^{1/4} \left(\frac{U_o t}{k_2 d_o}\right)^{1/2} \qquad (18)$$

Experimental evidence discussed in Part I on turbulent jet mixing suggests that:

- The macroscopically entrained air is first engulfed into large scale coherent structures and is subsequently cascaded down to the Kolmogorov scale.

- The mixing of the macroscopically entrained air is approximately uniform across the jet in a radial direction.

- The majority of the interface surfaces are generated just before the structures have reached the Kolmogorov scale. The interface surfaces are homogenized by molecular diffusion at this scale.

Based on the above experimental foundation, a simple turbulent diffusion flame model is postulated which contains only two major zones: the flame sheet and flame core. The flame sheet zone is the Kolmogorov scale structure which contains microscopically mixed fuel and air at a stoichiometric condition. The flame core zone consists of a mixture of the combustion products and the as-yet unreacted fuel which are molecularly mixed. After its formation, the flame sheet zone will subsequently conglomerate into the flame core structure via molecular diffusion process. Numerically, the flame sheet zone can be simulated by a well stirred reactor with proper characteristic residence time. The flame core zone can be represented by a plug flow reactor, which originally contains 100 percent raw fuel, and is continuously fed by the combustion products from the flame sheet reactor. In the meantime, the flame core zone also has to provide the flame sheet reactor with the rich mixture which contains a sufficient amount of raw fuel for stoichiometric combustion (corresponding to the rate of microscopic mixing of fresh air).

The idea defined above was illustrated in Figure 1-6 and is provided in a bit more detail as Figure 2-3. Quantification of the flow to each reactor is discussed below.

The rate of fresh air which is mixed into the flame sheet reactor can be computed by using Eqn. (16) and the rate of raw fuel to the reactor can be calculated by using Eqn. (17). The overall rate of mixture from the flame core reactor, which includes raw fuel and its diluent (combustion products), can be derived from Eqns. (16), (17), and (18), and expressed by

$$\frac{d}{dt}\left(\frac{\dot{m}_{fd}}{\dot{m}_o}\right) = \frac{1 k_3}{\Phi 2}\left(\frac{\rho_o}{\rho_m}\right)^{1/4}\left(\frac{U_o}{k_2 d_o t}\right)^{1/2}\left(\frac{1+ k_3\left(\frac{\rho_o}{\rho_m}\right)^{1/4}\left(\frac{U_o\, t}{k_2 d_o}\right)^{1/2}}{1 - \frac{k_3}{\Phi}\left(\frac{\rho_o}{\rho_m}\right)^{1/4}\left(\frac{U_o\, t}{k_2 d_o}\right)^{1/2}}\right)$$

The proper residence time for the flame sheet reactor corresponds to the molecular viscosity and the Kolmogoroff scale; i.e.,

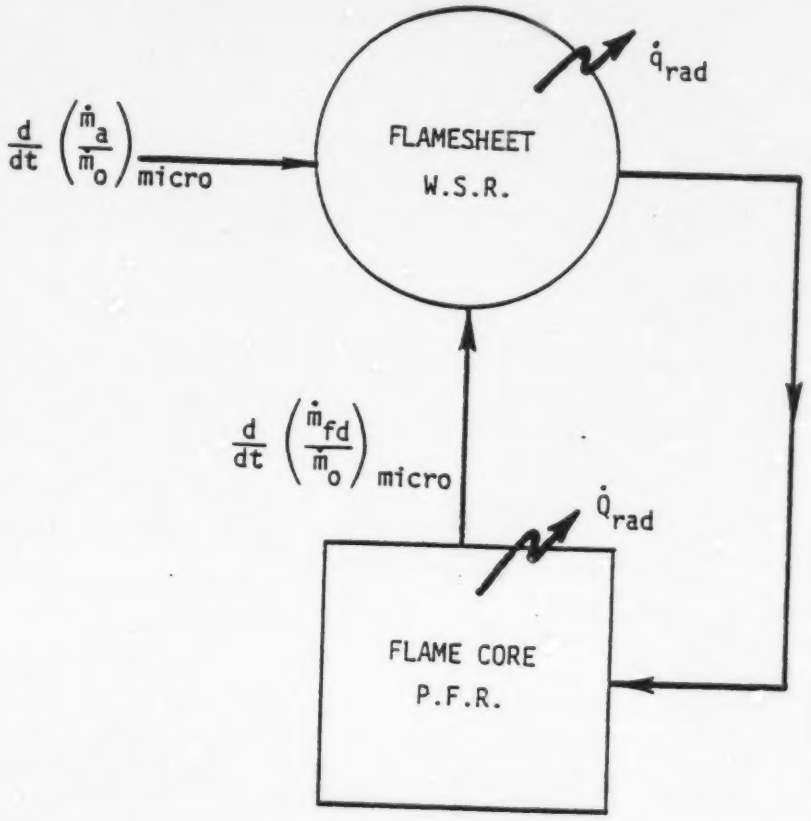

Figure 2-3. Schematic of Reactor Model.

$$\tau = C_1 \frac{\lambda^2}{\nu}$$

where C_1 is a proportional constant and ν is the kinematic viscosity. As discussed in Part I the Kolmogorov scale is evaluated by

$$\lambda = C_2 \left(\frac{\nu^3}{\varepsilon}\right)^{1/4}$$

where C_2 is another proportional constant. The rate of dissipation of turbulence is estimated by

$$\varepsilon = C_3 \frac{U_m^3}{d}$$

Thus, the characteristic residence time for the flame sheet reactor can be expressed by

$$\tau = \frac{C_1 C_2^2}{\sqrt{C_3}} \frac{\nu^{1/2} d^{1/2}}{U_m^{3/2}} \qquad (19)$$

Eliminating U_m by using Eqn. (12), the residence time expression becomes:

$$\tau = \beta \left(\frac{\rho_m}{\rho_o}\right)^{3/4} \left(\frac{4\, \nu^{1/2}\, k_2^2\, d_o^{1/2}}{U_o^{3/2}}\right) \left(\frac{X}{d_o}\right)^2 \qquad (20)$$

where $\beta \equiv C_1 C_2^2 / \sqrt{C_3}$ is a major physical uncertainty of the model. Expressing the residence time in terms of clock time by using Eqn. (14), we have

$$\tau = \beta\, 4 k_2 \left(\frac{\rho_m}{\rho_o}\right)^{1/4} \frac{t}{\sqrt{Re}} \qquad (21)$$

Reynolds number Re is defined as

$$Re = \frac{U_o d_o}{\nu}$$

where ν is the kinetmatic viscosity of the combustion products at typical flame temperatures. For CH_4/air flames ν is taken to be 1.2 cm^2/sec while for H_2/air flame ν is taken to be 4.0 cm^2/sec. Since the typical flame temperature is not known a prior, there is some uncertainty in ν. However, this uncertainty is minor and can be absorbed into the major certainty of the model, β.

II.3 Numerical Procedures and Heat Transfer Model

A computer code has been developed for the turbulent diffusion flame model which consists of a well stirred reactor and a plug flow reactor. The code was developed by making use of EER's existing one-dimensional reactor code. The numerical aspect of the diffusion flame model includes the following features:

- Implicit Finite Difference: The governing species and energy equations for both reactors are solved implicitly by backward finite difference formulation in time-like coordinate.

- Fully Detailed Kinetic Mechanism: The FCR I kinetic set consists of 181 elementary reactions and 36 species for CH_4/air flames which includes detailed NO and fuel nitrogen mechanisms. The kinetic set can be reduced to 17 species and 60 elementary reactions for H_2/air flames. (See Seeker, et. al, 1985 for details on kinetic reaction set.)

- Gas Radiative Heat Transfer: The radiative heat exchange between radiating gas and ambient is considered. The major radiating species in hydrocarbon flames are H_2O, CO_2 and CO. For small-scale gaseous flames, an optically thin approximation, which assumes that all the radiative energy from the flame escapes the flame envelope should be sufficiently accurate. For large-scale flames, self-absorption has to be considered. For modeling of simple turbulent jet diffusion flames, the axial dimension is much larger than the radial dimension and therefore, the radiative flux

in the axial direction tends to be absorbed while the radial radiative flux tends to escape. Richter (1974) has estimated the radial and axial energy flux for a typical turbulent diffusion flame by using the four-flux model. He concluded that only about 30 percent of the radiative energy radiates in the axial directon while 70 percent of the energy radiates radially. As a first order approximation in the current model, it is assumed that all the radiative flux in the axial direction will be self-absorbed while all the radiative flux in the radial direction will be lost to the ambient.

II.4 Sample Calculation and Sensitivity of Model Parameters

As the first example, which also serves to check out the correctness of the numerical procedures in the program, one of the CH_4/air turbulent diffusion flames measured by Bilger and Beck (1975), has been selected for simulation. This flame is a hydrogen jet issuing from a 0.635 cm nozzle into still air. The mean exit velocity is 19,323 cm/sec. Both hydrogen and air are initially at 300 K and at one atmosphere Pressure. The computer code was exercised for various values of β and the calculated NO concentration profiles* are shown in Figure 2-4. As illustrated, $\beta = 10$ gives the best agreement between prediction and experimental data. However, it should be noted that the universality of β requires further analytical and numerical studies.

In order to examine the sensitivity of the radiative heat transfer model on NO formation, computations were made for the particular flame by artificially varying the radiative heat transfer parameter, α, from 0.5 to 1.0. For example, $\alpha = 0.5$ means 50 percent self-absorption, while $\alpha = 1.0$ represents an optical-thin limit of heat loss. The results are plotted in Figure 2-5. To illustrate the impact of the heat transfer model on temperature, the profiles of the flame core temperature histories are plotted in Figure 2-6. No attempt was made to compare the calculated temperature profile against the measurements since temperature measurements give only the

---

* The computed NO concentration in the plots is the mean of instantaneous NO concentration from both reactors multiplied by k_1 which accounts for the dilution effect of macroscopic air.

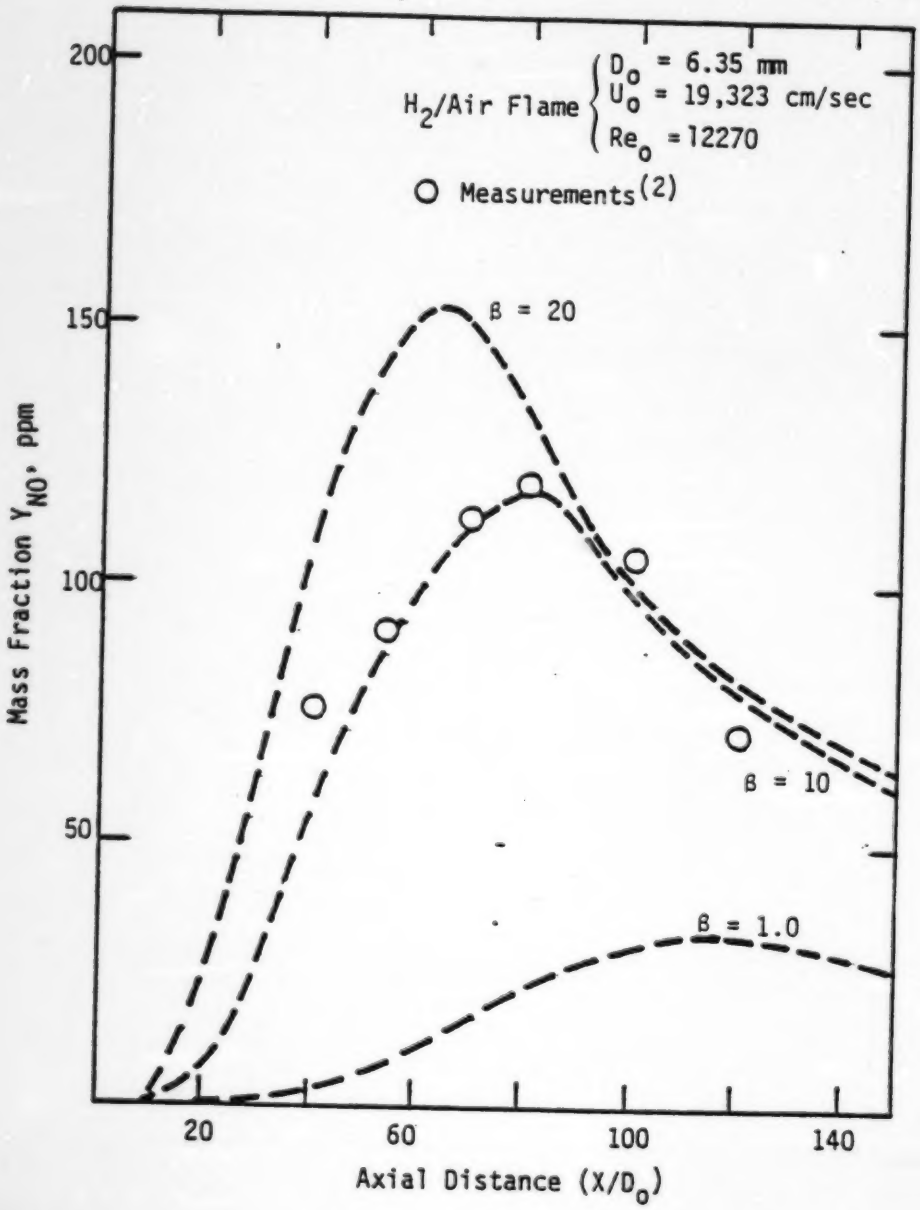

Figure 2-4. Sensitivity of β (α = 0.7).

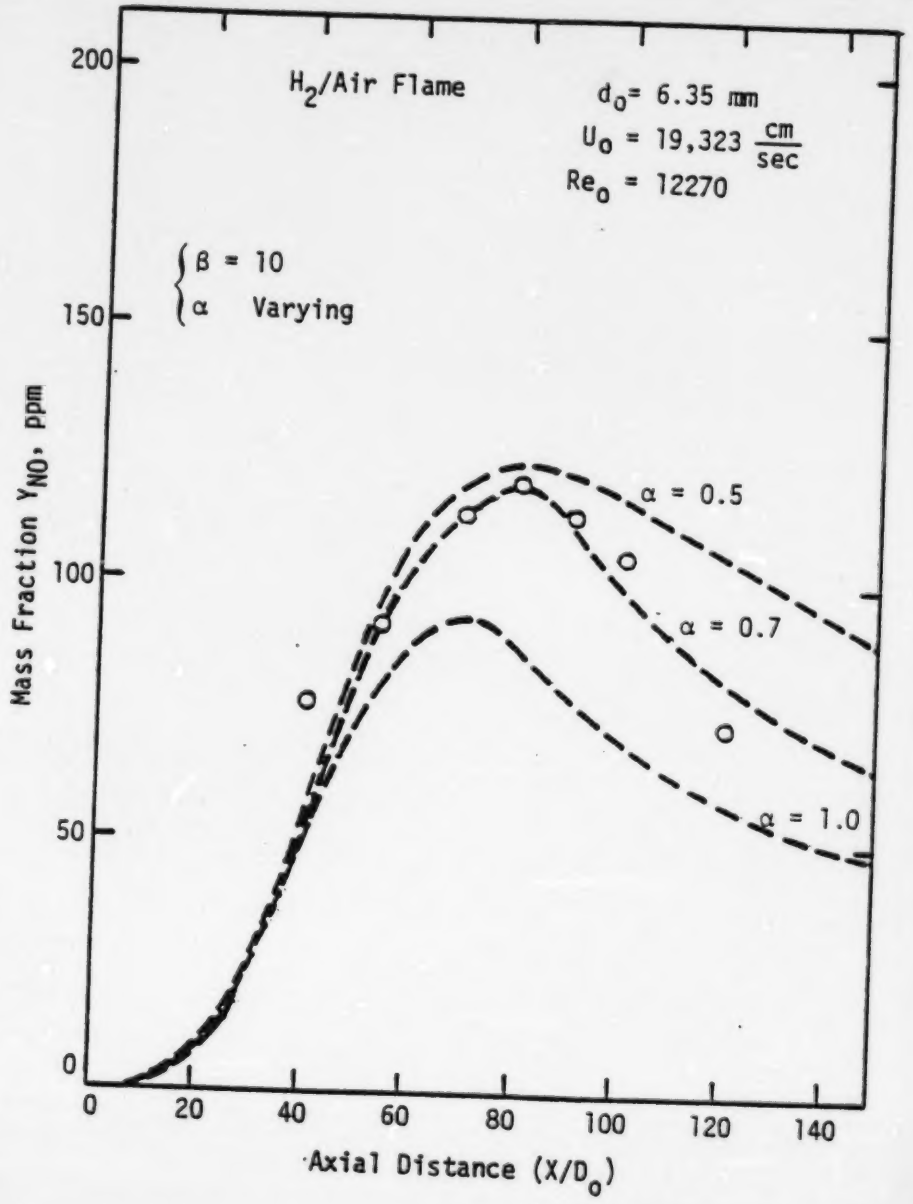

Figure 2-5. Sensitivity of Radiative Heat Transfer Parameter α (β = 10).

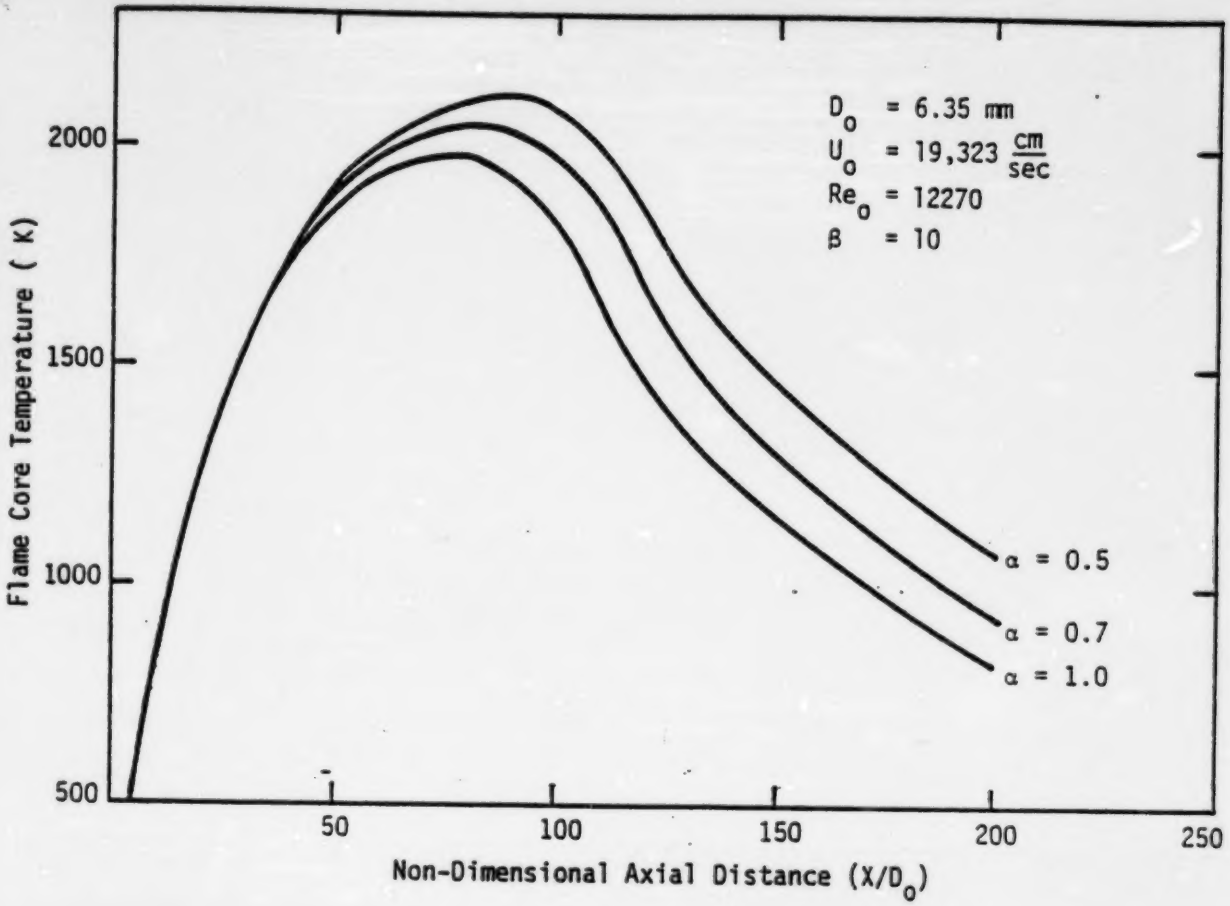

Figure 2-6. Effect of Radiative Heat Transfer on Flame Core Temperature History.

mean temperature of the macroscopic mixture which contains both the gases of the flame sheet and the flame core as well as the macromixed fresh air.

II.5 Comparison with Experimental Data and Discussion of Results

By setting $\beta = 10$, the model is used to predict the NO concentration of the various H_2/air flames reported by Bilger and Beck. (1975). The computed NO histories of three flames with constant Froude numbers (accomplished by varying U_o and d_o at the same time) are presented in Figure 2-7 and compared against the measured centerline NO concentrations. The agreements are encouraging. The same numerical results are also plotted differently in Figure 2-8 in terms of emission index per unit convective time, E/τ_o, versus Reynolds number of fuel jet, Re_o. The convective time scales, τ_o, is defined as the ratio of the nozzle diameter to the exit velocity. The emission index, E, is defined as the NO mass flux per unit of fuel mass flux. Figure 2-8 indicates a $(Re_o)^{-1/2}$ dependency of E/τ_o as was noted in the original paper by Bilger and Beck. However, it should be noted that when the Froude number (U_o^2/gd_o) is held constant, τ_o and Re_o are not mutually independent. Instead, τ_o is in proportion to $(Re_o)^{1/3}$, since by definition

$$Fr = \frac{U_o^2}{g\, d_o} \alpha \frac{(Re_o)^n}{(\tau_o)^m} = \frac{(U_o d_o/\nu_o)^n}{(d_o/U_o)^m} = \frac{(U_o)^{n+m}}{(\nu_o)^n (d_o)^{m-n}} \qquad (22)$$

Two equation can be developed for n and m,

$$n + m = 2$$

and

$$m - n = 1$$

thus requiring that

$$n = 1/2 \text{ and } m = 3/2$$

If Fr is held constant, then

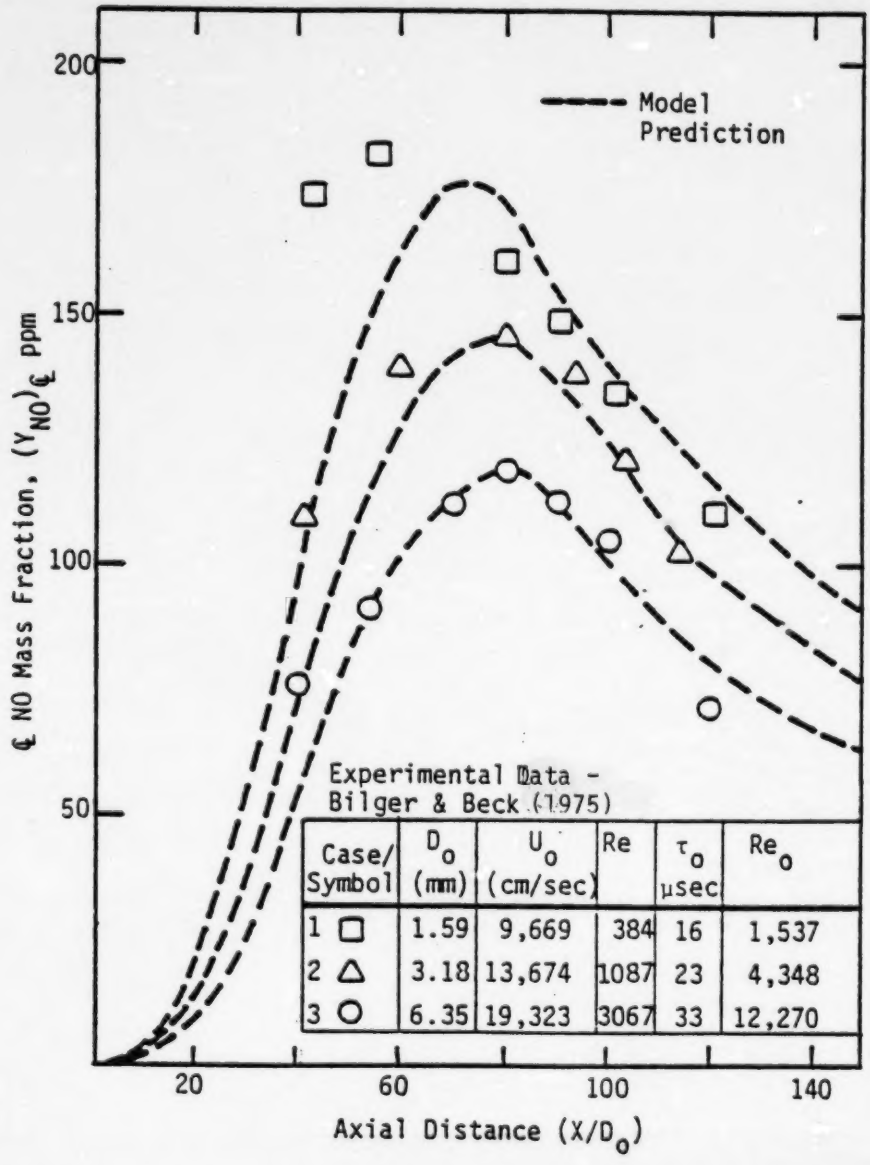
Model Prediction
Experimental Data - Bilger & Beck (1975)
Case/ Symbol | D_o (mm) | U_o (cm/sec) | Re | τ_o µsec | Re_o
1 □ | 1.59 | 9,669 | 384 | 16 | 1,537
2 △ | 3.18 | 13,674 | 1087 | 23 | 4,348
3 ○ | 6.35 | 19,323 | 3067 | 33 | 12,270
℄ NO Mass Fraction, $(Y_{NO})_{℄}$ ppm
200
150
100
50
20
60
100
140
Axial Distance (X/D_o)

Figure 2-7. Comparison of Model Calculated NO Against Measurements ($Fr = 6 \times 10^{-5}$) for H_2/Air Flames.

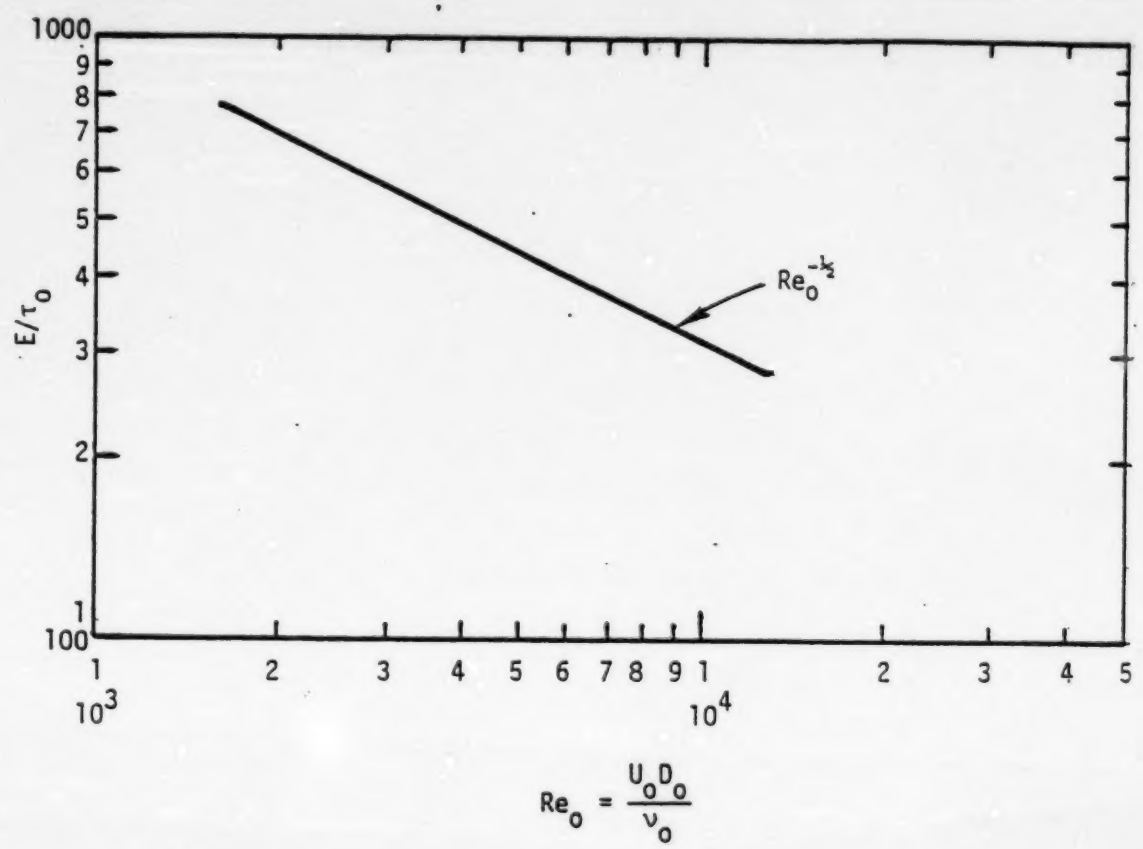

Figure 2-8. Predicted E/τ_o Against Re_o for H_2/Still Air Flames (at Constant Froude No., Fr = 6 x 10^5).

$$\tau_o \alpha Re_o^{1/3}$$

Furthermore, if we try to correlate E with τ_o and Re_o, we find that

$$E \alpha \frac{\tau_o^p}{Re_o^q} \text{ a } \frac{1}{(Re_o)^{q-p/3}} \qquad (23)$$

Since the data in Figure 8 shows $(Re)^{-1/2}$ dependency, we have:

$$E \alpha \frac{\tau_o}{(Re_o)^{1/2}} \alpha \frac{1}{(Re_o)^{1/6}} \qquad (24)$$

Thus the dependency of emission index (from Bilger and Beck, 1975) is actually -1/6. However, this type of correlation is meaningless since τ_o was not held constant.

Figure 2-9 shows the overall NO formation (mole/gm of fuel) in the flame sheet zone and flame core zone as functions of axial distance for flame No. 7 in Table 2-1 (Re_o = 12,270). The results indicate that NO is formed predominantly in flame sheet zone while approximately one third of that is destroyed in fuel-rich flame core zone.

Figure 2-10 shows the calculated NO emission index over a wide range of RE_o while holding τ_o constant (i.e., τ_o = 23 μsec). In the lower range of Re_o ($Re_o < 2 \times 10^4$) the emission index is insensitive to the increment of Re_o due to the following contradictory effects:

- Increasing Re reduces flamelet residence time and therefore reduces the time duration for NO kinetics.
- Increasing Re reduces flamelet residence time which in turn reduces flamelet radiation time and increases the flamelet temperature. This will increase the rate of NO formation.

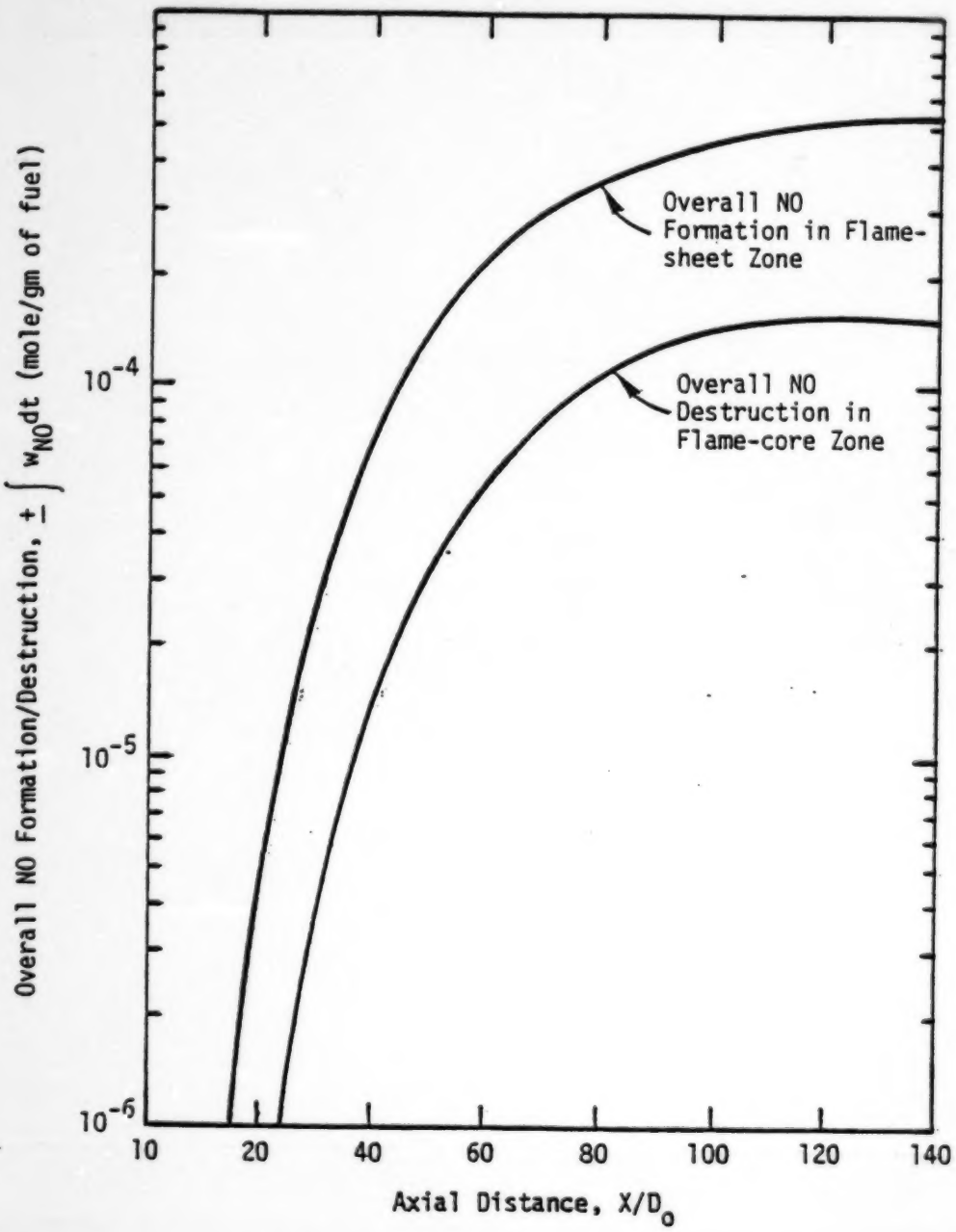

Figure 2-9. Overall NO Formation in Flame-sheet Zone and Overall NO Destruction in Flame-core Zone (Re_o = 12270, U_o = 19,323 cm/sec, D_o = 6.35 mm).

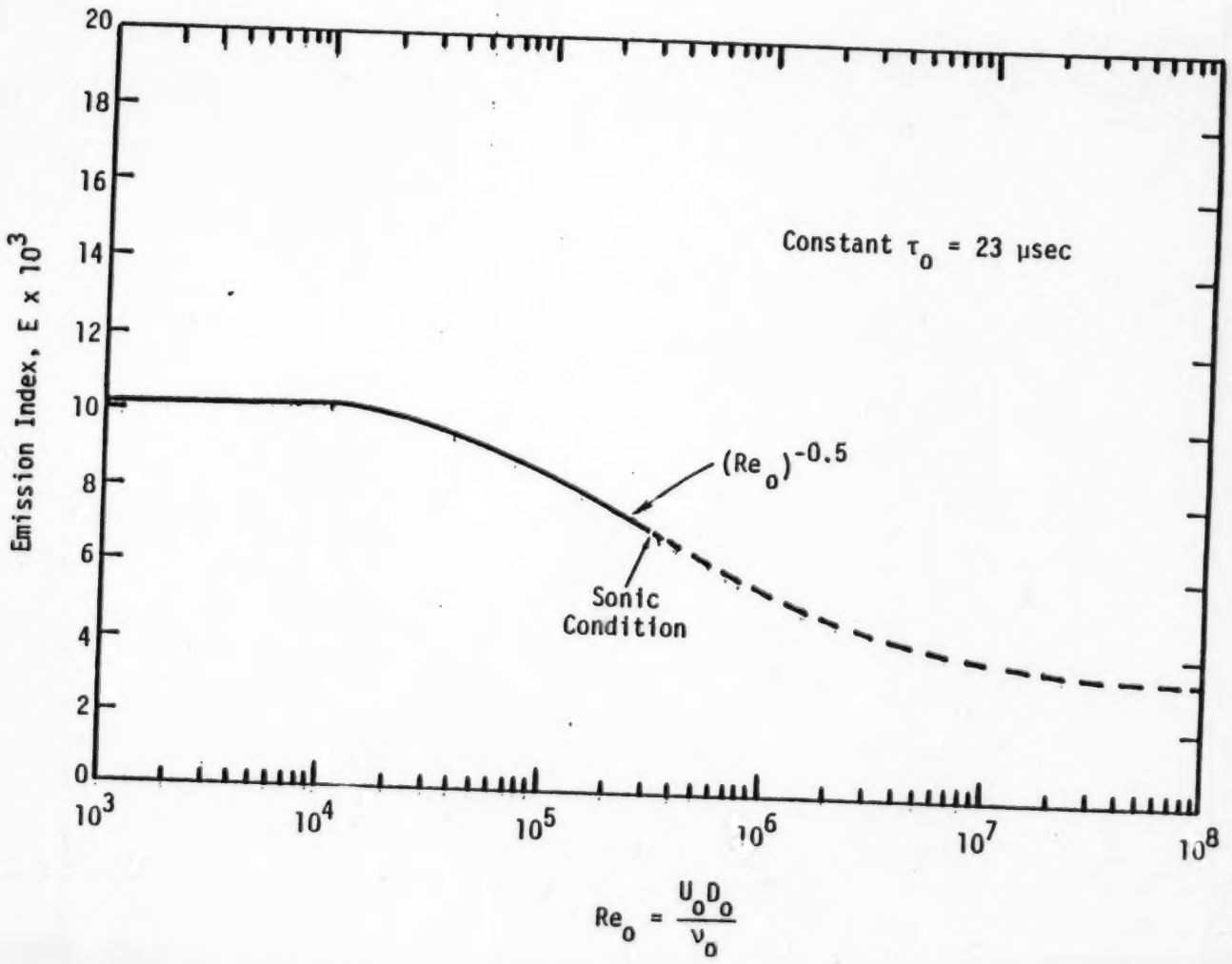

Figure 2-10. Emission Index Versus Re_o (H_2/Air Flame).

- Increasing Re reduces flamelet residence time and thus causes higher super-equilibrium radical pool concentration which will increase NO formation.

In the mid-Re_o range (Re_o = 2 x 10^4 ~ 10^6), the first effect is prevailing. Thus, the emission index is proportional to the flamelet residence time which, in turn, is proportional to $(Re_o)^{-1/2}$. In the very high Re_o range ($Re_o > 10^6$) the effect of the flame sheet is negligible due to short flame sheet residence time ($\tau << \tau_{no}$). NO is predominantly formed within the flame core zone where the equivalence ratio is close to unity (i.e., near the flame tip). The NO formation within this range is found to be proportional to convective time scale, but insensitive to Re_o.

Experimental data for free CH_4/air turbulent diffusion flames with NO measurements are very scarce. Recently Peters and Donnerhack (1981) have reported their experimental data on NO in CH_4/air flames. However, the experiment was performed in a co-flowing fuel-air system. The overall equivalence ratio of all flames was maintained at a constant value of 0.63 by varying air and CH_4 flow rates. The size of flame tube (external air tube) was fixed while the fuel nozzle diameter was varied. These flames are confined in nature, which limits the free supply of air for microscopic entrainment. The pressure gradient which occurs as a result of confinement could cause flow recirculation which in turn would affect the patterns of macroscopic entrainment and microscopic mixing. Techniques for treating confined flow are beyond the scope of this report. For the purpose of this report, we have selected only the flames from Peters and Donnerhack's data which are least affected by confinement. These flames are from the smallest fuel tubes which also have the highest fuel jet velocities and the lowest air velocities. The parameters of these flames and the emission indices are presented along with the results from the numerical model in Table 2. The predicted emission indices are within 15 percent of the measured value.

II.6 Concluding Remarks

A model has been formulated that describes, in a simple way, chemical reactions in turbulent fuel jets discharging into air. The model deals with both fast and slow reactions and is applicable therefore to nitric oxide generation processes.

Table 2-2. Comparison of Predicted and Measured Emission Indices for CH_4/Air Turbulent Diffusion Flame.

Flame No.	21	22	23	24
r_o (cm)	0.3	0.3	0.35	0.35
U_o (cm/sec)	2,070.	1,720.	1,780.	1,850.
Re_o	3,200.	2,630.	3,200.	3,340.
Fr	14,710.	10,000.	9,335.	10,000.
L_f/D_o	170.	157.	163.	171.
$(E)_{exp.} \times 10^3$	1.10	1.20	1.17	1.19
$(E)_{cal.} \times 10^3$	1.07	1.14	1.03	1.02

A basic aspect of the model is that molecular mixing which precedes the reaction does not take place as a consequence of the "turbulent diffusion" of the reactants towards each other down concentration gradients. Instead fuel and air are entrained throughout the jet, intertwine in large scale inviscid motions, and mix molecularly at the interfaces and as the mixture is homogenized at the Kolmogorov scale. This view of the mixing process leads to a model in which the state of the fuel-air mixture is independent of the radial coordinate. The usual bell-shaped distributions arise solely from the radial variation in the ratio of pure air to the fuel-air mixture.

Based on these concepts a numerical model has been developed and used to predict NO formation in simple turbulent diffusion flames. The results compare favorably against experimental data for both H_2/air and CH_4/air flames of various Reynolds numbers. The model results were found to be sensitive to a parameter β which influences the calculated residence time in the model's flame-sheet reactor zone. Encouraging results were achieved by empirically setting this parameter equal to 10. The model predictions are also sensitive to radiation heat transfer but a first order approximation, applicable to the simple flame types being models provided satisfactory comparisons to experimental data.

REFERENCES

Bilger, R.W. 1976 Turbulent jet diffusion flames, Pollution Formation and Destruction in Flames, Progress in Energy and Combustion Science, Chigier, ed., Vol. 1, p. 87, Pergamon Press.

Bilger, R.W. and Beck, R.E. 1975 Further experiments on turbulent jet diffusion flames, Fifteenth Symposium (International) on Combustion, p. 541, The Combustion Institute.

Broadwell, J.E. and Breidenthal, R.E. 1981 A simple model of mixing and chemical reaction in a turbulent shear layer, GALCIT Report FM81-10, California Institute of Technology.

Brown, G.L. and Roshko, A. 1974 On density effects and large structure in turbulent mixing layers, J. Fluid Mechanics, Vol. 64, No. 4, pp. 775-816.

Dimotakis, P.E., Miake-Lye, R.C., and Papantoniou, D.A. 1981 The structure and dynamics of round turbulent jets, XV International Symposium on Fluid Dynamics, Jachranka, Poland, also GALCIT Report FM82-01, California Institute of Technology.

Hawthorne, W. R., Weddell, D.S., and Hottel, H.C. 1949 Mixing and combustion in turbulent gas jets, Third Symposium on Combustion and Flame and Explosion Phenomena, p. 266, The William and Wilkins Company.

Hottel, H.C. 1953 Burning in laminar and turbulent fuel jets, Fourth Symposium (International) on Combustion, p. 97, The Williams and Wilkins Company.

Landau, L.D. and Lifshitz, E.M. 1959 Fluid Mechanics, Pergamon Press.

Marble, F.E. and Broadwell, J.E. 1977 The coherent flame model for turbulent chemical reactions, Project Squid Technical Report TRW-9-PU.

Marble, F.E. and Broadwell, J.E. 1980 A theoretical analysis of nitric oxide production in a methane/air turbulent diffusion flame, Interagency Energy/Environment R&D Report EPA-600/7-80-018 (NTIS PB80-218969).

Peters, N. and Donnerhack, S. 1981 Structure and similarity of nitric oxide production in turbulent diffusion flames, Eighteenth Symposium (International) on Combustion, p. 33, The Combustion Institute.

Richer, W. and R. Quack, "A Mathematical Model of Low-Volatile Pulverized Fuel Flame," Heat Transfer in Flames, Chapter 5, 1974.

Ricou, F.P. and Spalding, D.B. 1961 Measurements of entrainment by axisymmetrical turbulent jets, J. Fluid Mechanics 11, 21.

Roshko, A. 1977 "Structure of Turbulent Shear Flows: A New Look," AIAA Journal, Vol. 14, pp. 1349-1357 and Vol. 15, p. 768.

Seeker, W.R., Heap, M.P., Tyson, T.J., Kramlich, J.C. and Corley, T.L. 1985 Fundamental Combustion Research Applied to Pollution Formation, Volume I, FCR Program Overview and Gas Phase Chemistry, EPA-600/7-85-048 (NTIS PB86-122660).

Spalding, D.B. 1978 A general theory of turbulent combustion, The J. of Energy 2(1), p. 16.

Tennekes, H. and Lumley, J.L. 1972 A First Course in Turbulence, The MIT Press.

Uberoi, M.S. and Singh, P.I. 1975 Turbulent mixing in a two-dimensional jet, The Physics of Fluids 18(7).

Weddell, D.S. 1941 Turbulent Mixing in Gas Flames and Its Reproduction in Liquid Models, Doctor of Science Dissertation, Massachusetts Institute of Technology.

Witte, A.B. et al. 1974 Aerodynamic reactive flow studies of the H_2F_2 laser, II, Air Force Weapons Lab, Kirtland AFB, New Mexico, AFWL-TE-74-78.